SECOND EUROPEAN CONFERENCE ON EARTHQUAKE ENGINEERING
AND SEISMOLOGY, ISTANBUL AUG. 25-29, 2014

GRAVITY LOAD COLLAPSE OF REINFORCED CONCRETE COLUMNS WITH DECREASED AXIAL LOAD

Takaya NAKAMURA[1] and Manabu YOSHIMURA[2]

ABSTRACT

When reinforced concrete (RC) columns reach near-collapse and undergo axial shortening following shear failure, some of the axial load sustained by the columns is transferred to neighboring columns, thus, decreasing the axial load of the columns that are near collapse. This study examines the effect of decreased axial load on collapse behavior. Full-scale column specimens with shear failure mode were tested under decreased axial load or constant axial load until they collapsed. The effects of varied rates of axial load decrease on column collapse drift were studied, and computed and observed collapse drifts were compared.

INTRODUCTION

The loss of axial load carrying capacity or gravity load collapse in reinforced concrete (RC) columns is one of the most dangerous forms of damage that RC buildings suffer during earthquakes. During previous severe earthquakes, several RC buildings suffered story collapse owing to gravity load collapse of columns following shear failure. However, in several cases, the columns themselves did not collapse completely (Fig. 1) despite suffering severe damage following shear failure. When columns are on the verge of collapsing, some of the axial load sustained by them is transferred to neighboring durable columns through girders (Fig. 2), i.e., the axial load that the RC columns are subjected to decreases when undergoing axial shortening owing to shear failure. Therefore, the structural performance of the columns improves.

In the past, for revealing the collapse behavior of RC columns, collapse tests were performed on columns with constant axial load (Moehle et al., 2000 and Nakamura et al., 2003), but collapse tests with decreased axial load are yet to be conducted. Axial load decrease was confirmed in a test for RC frame structure (Elwood et al., 2003); however, the effect of decreased axial load on the lateral drift of columns during collapse are yet to be studied. This study aims to examine the effects of variable rates of axial load decrease on the column collapse drift with shear failure mode. We attempted to predict the collapse drift using an empirical equation. The results are useful in detailed evaluation of the seismic performance of RC columns.

[1] Associate Professor, Niigata University, Niigata, takaya@eng.niigata-u.ac.jp
[2] Professor, Tokyo Metropolitan University, Tokyo, yoshimura@tmu.ac.jp

Figure 1. RC column whose axial load might decrease, 1995 Kobe earthquake (AIJ, 1997)

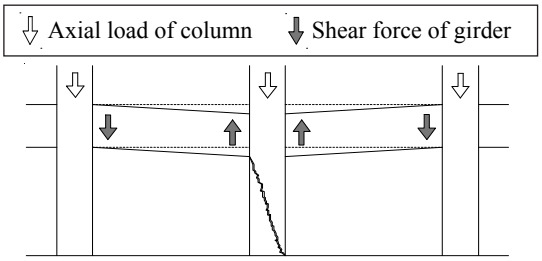

Figure 2. Mechanism of the axial load decrease

OUTLINE OF TEST

(1) Specimen

Sixteen full-scale column specimens were fabricated and designed to ensure shear failure. Table 1 presents the specimens' structural properties. As presented in Table 1, Series SA, SB, SC, S, and L were considered. As examples, the reinforcement details and the column sections of the specimens for Series SB, S, and L are illustrated in Figs. 3 and 4. The column heights were 900 mm and 1400 mm, each column section was 450 mm × 450 mm, and the height-to-depth ratio was 2.0: 3.1. The transverse bar ratios (p_w) were 0.11%, 0.16%, 0.21%, and 0.42%. The longitudinal bar ratios (p_g), defined as the total main reinforcement areas divided by the column section, were 1.13%, 1.70%, and 2.30%. Table 2 presents the material properties. Normal reinforcement and concrete were used.

The axial stress ratios (η) were 0.16 and 0.18 times the concrete strength multiplied by the column section. For the specimens with decreased axial load, η decreased between 25–75% of the initial values in the midst of loading. In each series, the specimens with constant and decreased axial load were compared. The specification was as follows. For Series SA, SB, and SC, the initial value of η was 0.16, which was then decreased to 0.08 (100–50%). For Series S, the initial value η = 0.18 decreased to 0.11 (100–60%), 0.07 (100–40%), and 0.04 (100–20%), and for Series L, the initial value η = 0.18 decreased to 0.14 (100–75%) and 0.09 (100–50%).

Table 3 lists the shear and flexure strengths computed for each specimen by the conventional equation in Japan (Architectural Institute of Japan, 1991).

Table 1. Specimen structural properties

Name	Series	Width×depth b × D (mm × mm)	Height h_0 (mm)	h_0/D	Longitudinal bar ratio[1] p_g (%)	Transverse bar ratio p_w (%)	Axial stress ratio[2] η	Loading
A1	Series SA	450 × 450	900	2.0	1.13 (8-D19)	0.11 (2-D10@300)	Constant (0.16)	Cyclic
A2							Decreased (100%→50%)	
B1	Series SB				1.70 (12-D19)	0.21 (2-D10@150)	Constant (0.16)	Monotonic
B2							Decreased (100%→50%)	
B3							Decreased (100%→50%)	
B4							Constant (0.16)	Cyclic
B5							Decreased (100%→50%)	
C1	Series SC				2.30 (12-D22)	0.42 (2-D10@75)	Constant (0.16)	Cyclic
C2							Decreased (100%→50%)	
S100	Series S				1.70 (12-D19)	0.21 (2-D10@150)	Constant (0.18)	Cyclic
S60							Decreased (100%→60%)	
S40							Decreased (100%→40%)	
S20							Decreased (100%→20%)	
L100	Series L		1400	3.1		0.16 (2-D10@200)	Constant (0.18)	
L75							Decreased (100%→75%)	
L50							Decreased (100%→50%)	

(1) Numeral after D denotes bar diameter in mm. (2) Axial stress ratio, $\eta_c = N / (b \cdot D \cdot \sigma_B)$, (N: axial load)

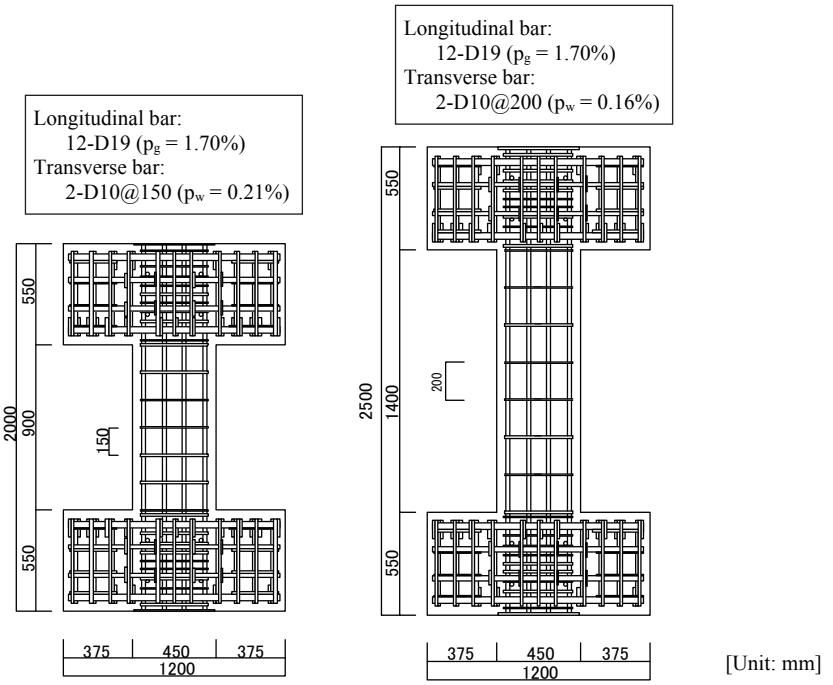

Series SB and S Series L

Figure 3. Reinforcement details

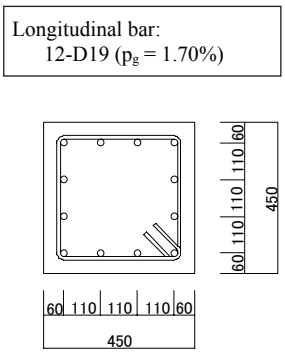

Series SB, S, and L

Figure 4. Column section

Table 2. Material properties

(a) Steel

	Yield stress (N/mm^2)	Strain at yield stress (%)
D22	376	0.28
D19	383	0.25
D10	399	0.25

(b) Concrete

	Max. stress σ_B (N/mm^2)
Series SA, SB, SC	28.0
Series S, L	25.0

Table 3. Computed strength

Name	Series	Shear strength (kN)	Flexure strength (kN)	Shear/Flexure
A1, A2	Series SA	406	607	0.66
B1, B2, B3, B4, B5	Series SB	457	731	0.61
C1, C2	Series SC	526	859	0.61
S100, S60, S40, S20	Series S	508	750	0.68
L100, L75, L50	Series L	385	482	0.80

(2) Loading method

Fig. 5 illustrates the test apparatus. A pantograph was placed to prohibit the loading beam on the column top from rotating (to realize double-curvature deformation). The specimens were laterally loaded by a lateral actuator under constant or decreased axial load, applied by a vertical actuator. The vertical actuator controlled the load, and the lateral actuator controlled the displacement. The tests were terminated by the vertical actuator limiter, which was set to operate when the collapse initiated and axial deformation reached 50 mm (Series SA, SB, and SB) and 80 mm (Series S and L).

As for the loading history, we used monotonic and cyclic loadings. The reason for including monotonic loading was that in the pseudo dynamic tests of Kobe earthquake motions, lateral drifts were observed to shift in lateral direction (Nakamura el al., 2012). Fig. 6 illustrates the detailed loading history used for the cyclic loading. All specimens except L100 were finally loaded to the

positive direction as long as the axial load could be maintained. Only L100 collapsed during cyclic loading.

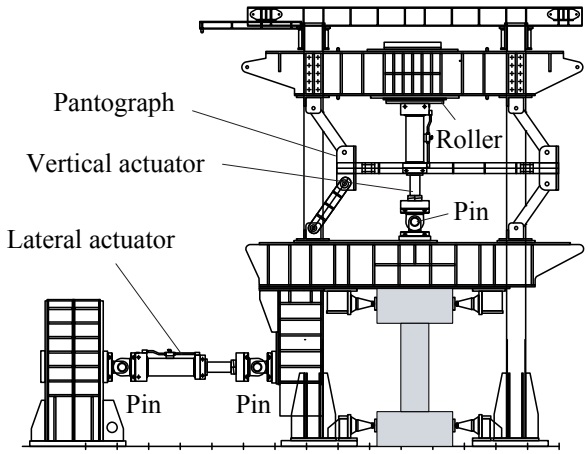

Figure 5. Test apparatus

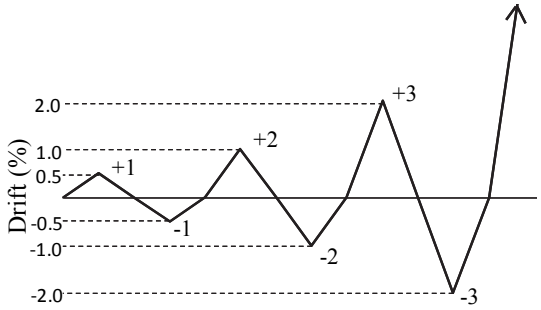

Figure 6. Loading history (cyclic)

(3) Axial load decreasing point

Axial load decreased following shear failure presumably owing to the large axial shortening of the column. Fig. 7 illustrates the axial deformation and lateral drift relation for specimen S100. In Fig. 7, the triangle mark indicates the appearance of the first shear crack, and the square mark indicates the collapse. As presented in Fig. 7, at the shear crack, the axial deformation was still small. Thereafter, the axial deformation rapidly increased when the column reached near-collapse. Thus, in the performed tests, the axial loads decreased when the specimens were near collapsing, where they underwent large axial shortening attributed to shear failure. For specimen B2 alone, the axial load was decreased at the point immediately after the appearance of the shear crack. Thus, specimen B2 was compared to specimen B3 whose axial load decreased at near-collapse. The points of axial load decrease for each specimen are plotted in Figs. 8 and 9.

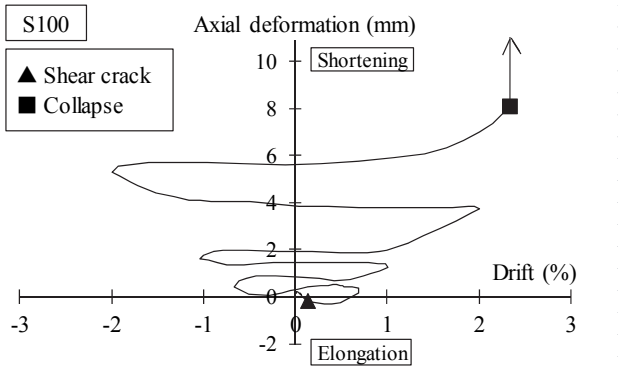

Figure 7. Axial deformation vs. drift (Specimen S100)

TEST RESULTS

All specimens failed in shear, and most of them finally lost their axial load-carrying capacity. In this study, “collapse” is the column’s loss of axial load-carrying capacity and “collapse drift” is the maximum lateral drift experienced prior to collapse. The test results are presented in Table 4.

Fig. 8 illustrates the lateral load and lateral drift relations; the lateral drift is divided by the column height. Fig. 9 shows the axial deformation and lateral drift relations. Figs. 8 and 9 are the skeleton curve of the positive direction where the collapse occurred, except in the case of L100. Fig. 10 shows the damage states observed at the drift of +1.0% and after collapse for S100 and L100. For

all specimens except A2, B3, C2, and S20, when the collapse occurred, the axial deformation suddenly increased and the test was terminated by the limiter of the vertical actuator. For A2, B3, C2, and S20, even though the sudden axial shortening did not occur until the axial deformation reached the limiter, we regarded the lateral drift at the final step as the collapse drift, because the column was assumed to be on the edge of collapsing due to its large axial deformation.

Collapse behavior is stated below for comparison of A1 and A2 (Series SA), and comparison of L100, L75, and L50 (Series L).

A1 and A2

Fig. 8(a) compares the lateral load and lateral drift relation for specimens A1 and A2. The two specimens have the same reinforcement details and loading histories, but the loading method of the axial load differed (A1: constant axial load; A2: decreased axial load). In Fig. 8(a), the triangle marks the point where the axial load was decreased, and each square marks the collapse. As presented in Fig. 8(a), both specimens collapsed when the lateral load decreased to approximately zero. At the moment of collapse, fracture of the transverse bar and loosening at the hook as well as buckling of the longitudinal reinforcements were observed. Similar behavior was observed at the collapse of the other specimens. As illustrated in Figs. 8(a) and 9(a), the strength reduction and axial deformation increase of A2 after the axial load decrease was smaller than in the case of A1 with constant axial load. The collapse drift of specimen A1 was 1.95% and that of specimen A2 was 11.8%. The latter was 6.1 times larger than the former. This rate is discussed later as "increased rate of collapse drift." The collapse drift was greater for columns with decreased axial load than for those with constant axial load. Similar behavior was observed for other series.

L100, L75, and L50

These specimens have the same reinforcement details and loading histories, but the loading method of the axial load differed (L100: constant axial load; L75 and L50: decreased axial load). Fig. 8(e) compares the lateral load and lateral drift relations for specimens L100, L75, and L50. Note that L100 was the only specimen that collapsed during cyclic loading. According to the definition of collapse drift, the collapse drift of L100 was 2.0%. The collapse drifts of L75 and L50 were 5.89% and 11.7%, respectively. The collapse drifts of L75 and L50 were 2.9 and 11.7 times larger than that of L100, respectively. As illustrated in Figs. 8(e) and 9(e), the larger the axial load decrease, the smaller is the strength reduction and the axial deformation increase. Thus, the larger the axial load decrease, the larger is the collapse drift.

Table 4. Test results

Name	Series	Maximum load (kN)	Drift at maximum load (%)	Drift at axial load decrease (%)	Axial deformation at axial load decrease (mm)	Collapse drift (%)	Axial deformation at collapse (mm)
A1	Series SA	570	0.29	—	—	1.95	8.17
A2		557	0.26	1.03	2.07	11.8	50.1
B1	Series SB	594	0.50	—	—	5.46	15.3
B2		607	0.36	0.97	0.13	18.9	44.2
B3		545	0.66	4.03	7.77	11.6	48.8
B4		578	0.50	—	—	3.68	9.38
B5		565	0.24	3.02	6.57	8.46	25.3
C1	Series SC	687	0.68	—	—	12.0	25.0
C2		715	0.93	11.1	17.8	19.2	50.0
S100	Series S	522	0.14	—	—	2.34	8.11
S60		577	0.40	3.50	5.12	10.5	19.5
S40		505	0.44	3.01	5.24	9.23	20.0
S20		562	0.28	2.19	4.51	23.0	80.0
L100	Series L	506	0.82	—	—	2.00	59.3
L75		526	0.90	1.34	0.54	5.89	16.5
L50		497	0.69	1.20	0.72	11.7	26.5

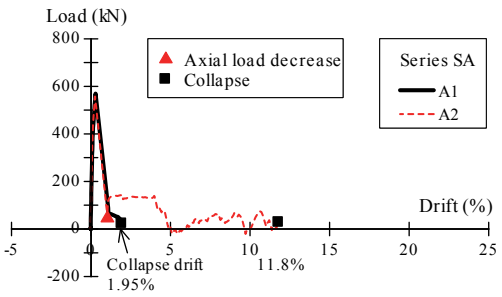

(a) Series SA

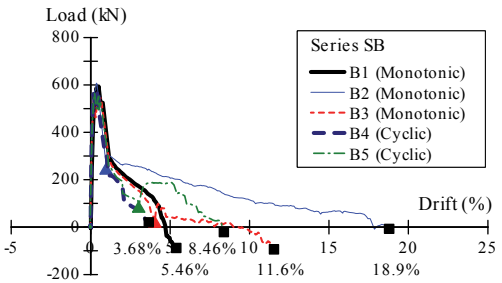

(b) Series SB

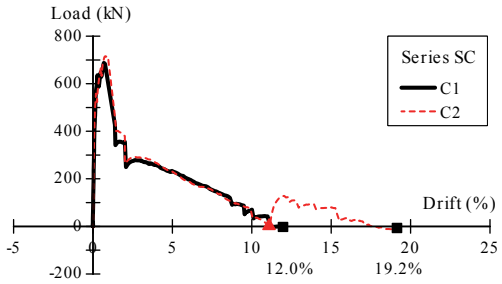

(c) Series SC

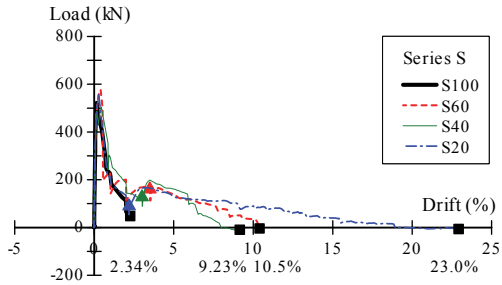

(d) Series S

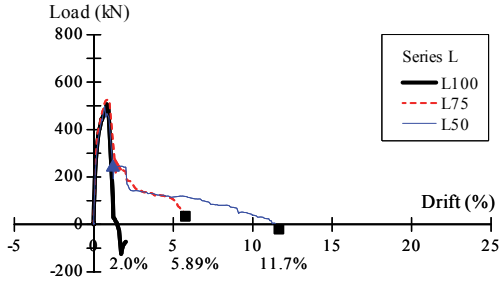

(e) Series L

Figure 8. Load vs. drift

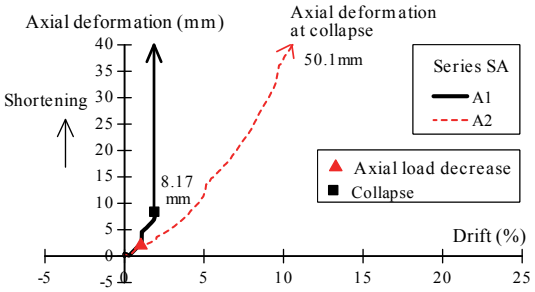

(a) Series SA

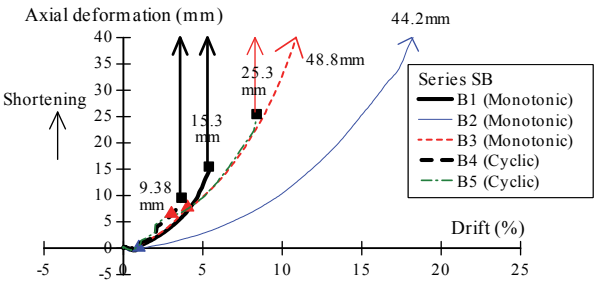

(b) Series SB

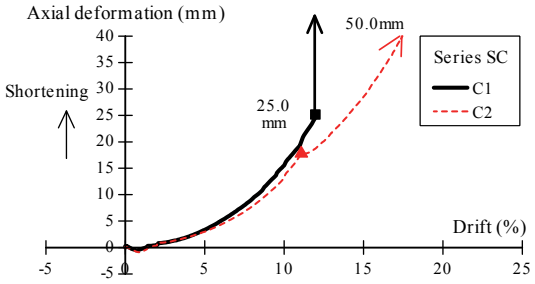

(c) Series SC

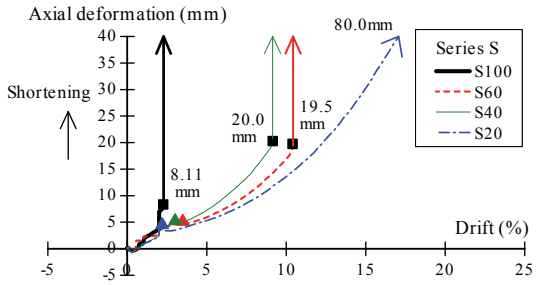

(d) Series S

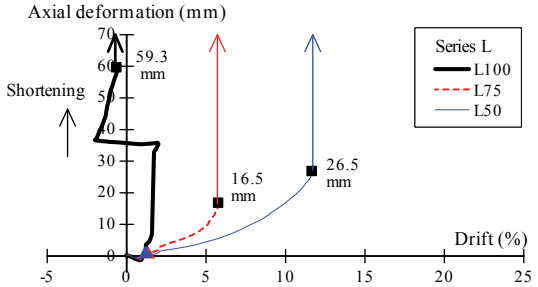

(e) Series L

Figure 9. Axial deformation vs. drift

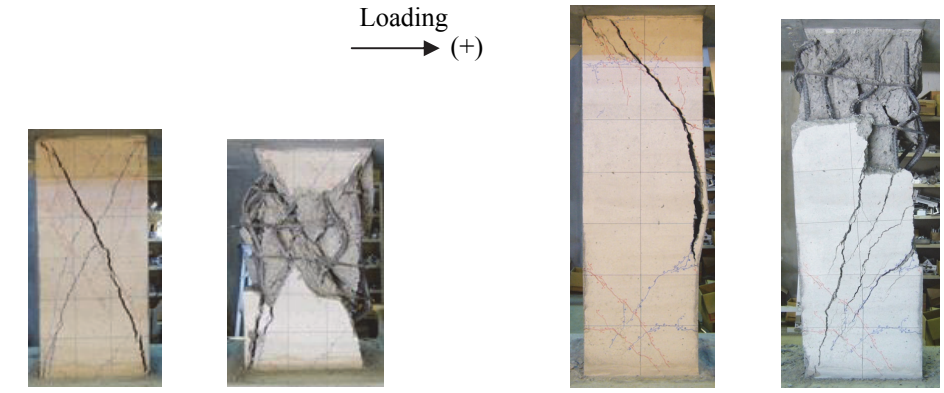

(a) S100 (b) L100

Figure 10. Damage states

DISCUSSION

(1) Effect of axial load decreasing point on collapse drift

As illustrated in Fig. 8(b), the collapse drift of specimen B2, whose axial load decreased at the point immediately after the shear crack appearance, was 18.9%. The collapse drift of specimen B3, whose axial load decreased at near-collapse, was 11.6%. The former was 1.6 times larger than the latter. The axial load decreasing point influences the collapse behavior. Thus, the sooner the axial load decreases, the greater the collapse drift will be.

(2) Increased rate of collapse drift

Fig. 11 indicates the increased rate of collapse drift, which is the ratio of a specimen's collapse drift with decreased axial load to that with constant axial load, for each of the specimens. The vertical axis in Fig. 11 represents the axial load decreasing rate, which is defined as the ratio of the axial load after decreasing to the initial axial load. As the rate decreases, the axial load decreases further. As illustrated in Fig. 11, the greater the axial load decrease, the larger the collapse drift. Specifically, when the axial load decreased to 75%, 50% (40–60%), and 20%, the collapse drift was approximately three, two to six, and ten times more than that of the specimens with constant axial load, respectively.

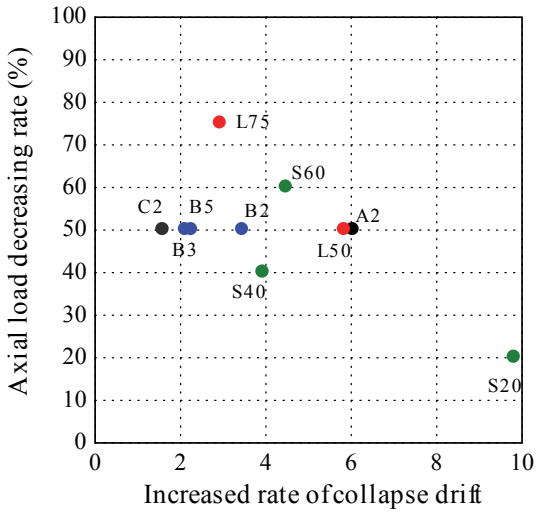

Figure 11. Increased rate of collapse drift

(3) Effect of test variables on collapse drift

The collapse drift ranges from 1.95% to 23.0% (Table 4). The effect of the test variables on the collapse drift is discussed below.

Effect of loading history

As illustrated in Fig. 8(b), the collapse drifts were smaller for the cyclic specimens (B4 and B5) than for the monotonic ones (B1 and B3) when under the same axial loading method (constant or decreasing). B2, with an axial load decreasing point that differs from those of the other specimens, is excluded. The collapse drift is compared in Fig. 12 with respect to the loading history. The ratios of collapse drift in the cyclic and monotonic case are 0.67 and 0.73, respectively. Thus, the ratios were almost the same, irrespective of the axial loading method.

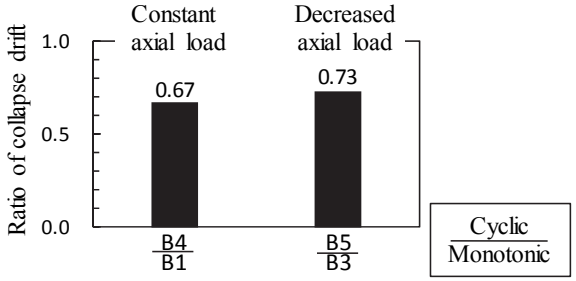

Figure 12. Comparison of collapse drift with respect to loading history

Effect of axial load

Fig. 13 illustrates collapse drift vs. axial stress ratio (η) relations for all specimens. In Fig. 13(a), the horizontal axis for specimens with decreased axial load is the axial stress ratio prior to decreasing. According to Fig. 13(a), collapse drifts vary widely for the same η. By contrast, In Fig. 13(b), the horizontal axis for specimens with decreased axial load is the axial stress ratio post decreasing. According to Fig. 13(b), there is a correlation between the collapse drift and η. This result indicates that the near-collapse axial load (decreased axial load) significantly affects the collapse drift. However, in Fig. 13(b), collapse drifts vary slightly for the same η (points in the dashed circle). This will be discussed in the next paragraph.

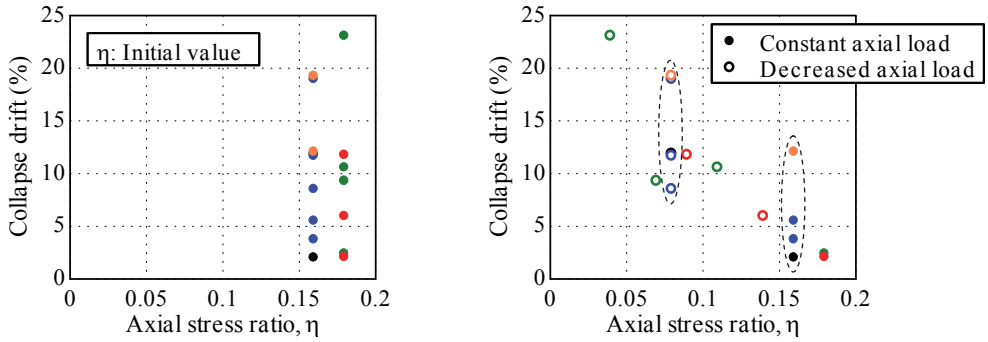

(a) η: before decreasing (b) η: after decreasing

Figure 13. Collapse drift vs. axial stress ratio (η)

Effect of longitudinal bar ratio

Fig. 14 illustrates collapse drift vs. longitudinal bar ratio (p_g) relations for the specimens with the same near-collapse axial load (Fig. 13(b), points in the dashed circle). Fig. 14(a) illustrates the relation for the specimens with constant axial load (η = 0.16), all of which have the same loading history (cyclic). Fig. 14(b) illustrates the relation for the specimens with decreased axial load (η = 0.08), all of which have the same loading history (cyclic). According to Fig. 14(a) and (b), the collapse drift becomes smaller as the longitudinal bar ratio decreases. This result agrees with a past study by Nakamura et al. (2003). Note that the reason behind the relation between A2 and B5 was different is unclear. As stated in a previous study (Yoshimura, 2008), the effect of the longitudinal bar ratio was the decrease of compression capacity of these bars because of the local flexural deformation near the shear crack. Thus, for the shear columns, the large amount of longitudinal bars is advantageous because collapse is controlled by the longitudinal bars.

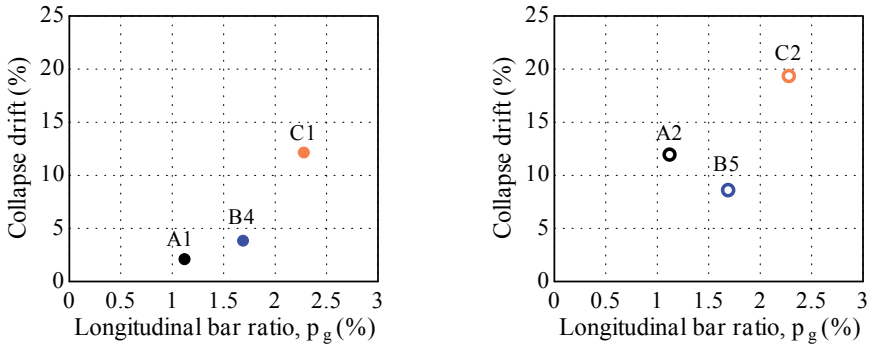

(a) η = 0.16 (constant axial load) (b) η = 0.08 (decreased axial load)

Figure 14. Collapse drift vs. longitudinal bar ratio (p_g)

(4) Evaluation of collapse drift

We attempted to predict the collapse drift using an empirical equation (Ito et al., 2011). The equation computes the collapse drift ($_cR_u$) of a shear-failing column using three values: the transverse bar ratio (p_w), the longitudinal bar ratio (p_g), and the axial stress ratio (η). These values significantly affect the collapse drift.

$$cRu = 22.42 \cdot p_w + 4.57 \cdot p_g - 51.27 \cdot \eta + 1.52 \geq 1.5 \quad (1)$$

where $_cR_u$, p_w, and p_g are percentages (%).

The equation was based on the test results where the column specimens were only loaded under constant axial load. Thus, it is unclear whether the collapse drift of the columns with decreased axial load can be evaluated using this equation. Fig. 15 compares the observed collapse drifts ($_eR_u$) and the computed ones. In Fig. 15, the specimens with constant axial load are underlined. In case of the specimens with decreased axial load, the collapse drift was computed using both initial and decreased axial load. Table 5 shows the average values and coefficients of variation of $_eR_u/_cR_u$. For the specimens with constant axial load, the average value and coefficient of variation are 0.82 and 0.32, respectively. In this case, the computed collapse drifts agree with the observed ones. If the initial axial load is used for specimens with decreased axial load, the average value and coefficient of variation are 3.11 and 0.62, respectively. However, if the decreased axial load is used, the average value and coefficient of variation are 1.41 and 0.34, respectively. According to Fig. 15 and Table 5, the computed collapse drifts agree with the observed ones if the decreased axial load is used. This result suggests, that the near-collapse axial load (decreased axial load) significantly affects the collapse drift.

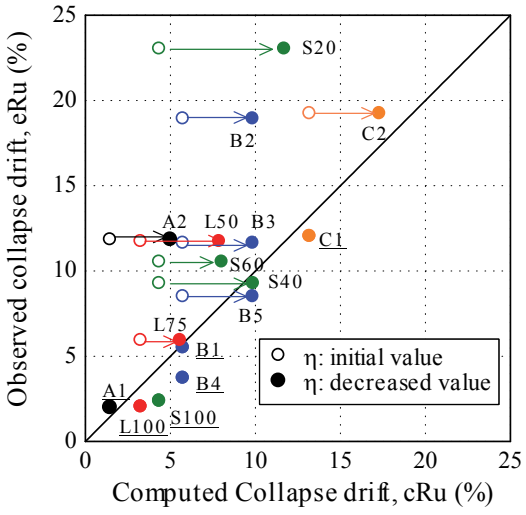

Figure 15. Observed verses computed collapse drift

Table 5. Average value and coefficient of variation of ${}_eR_u/{}_cR_u$

	Specimens with constant axial load	Specimens with decreased axial load	
		η: initial value	η: decreased value
Average value	0.82	3.11	1.41
Coefficient of variation	0.32	0.62	0.34

(5) Axial deformation at collapse vs. collapse drift relations

A previous research has attempted to formulate the post-peak behavior of RC columns, until gravity load collapses, using the measured residual axial deformation after earthquakes (Yoshimura, 2008). The method requires the axial deformation at collapse vs. collapse drift relation. The study reported that the average ratio of the axial deformation at collapse to the collapse drift was 0.22 (Yoshimura et al., 2005). Note that the study was based on test results where the column specimens were loaded only under constant axial load. Thus, whether the relation can be applied to columns with decreased axial load is unclear.

Fig. 16 illustrates the axial deformation at collapse vs. collapse drift relations for specimens in this paper. The axial deformations are divided by the column height. L100, which collapsed during cyclic loading, is excluded. According to Fig. 16, the axial deformation at collapse increases linearly with the increase in collapse drift. The average ratio of the axial deformation at collapse to the collapse drift was 0.31, irrespective of the axial loading method (constant or decreasing). However, the reason behind the average ratio being larger than the value of 0.22 from the past study was unclear.

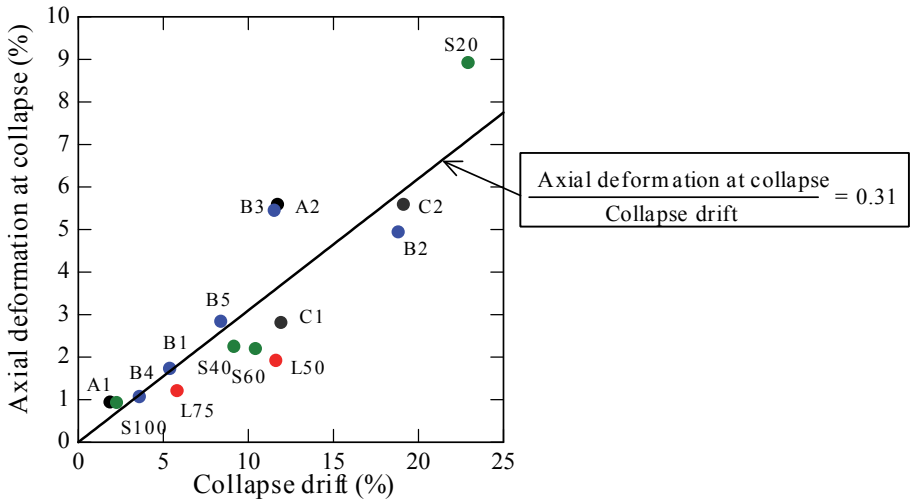

Figure 16. Axial deformation at collapse vs. collapse drift

CONCLUSIONS

We examined the effect of decreased axial load on the collapse drift of RC columns. The major findings of this study are as follows.

1) Columns for which the initial axial load decreased show larger collapse drift than those for which the initial axial load was kept constant.
2) The greater the axial load decrease, the larger is the collapse drift. Specifically, when the axial load decreased to 75%, 50% (40%–60%), and 20%, the collapse drift was approximately three, two to six, and ten times more than that of specimens with constant axial load, respectively.
3) For the columns with decreased axial load, the computed and observed collapse drifts agree if the decreased axial load is used in the equation of the collapse drift.

4) The axial deformation at collapse increases linearly with the increase in collapse drift. The average ratio of axial deformation at collapse to collapse drift is 0.31, irrespective of the axial loading method (constant or decreasing).
5) The axial load decreasing point influences collapse behavior. The sooner the axial load decreases, the greater is the collapse drift.

ACKNOWLEDGEMENT

The authors express their gratitude to Mr. Kazuhiro Shiroishi, Satoru Muto, and Sho Ito, former students of Tokyo Metropolitan University, for their assistance.

This work was supported by JSPS Grants-in-Aid for Scientific Research Grant: Number 21360269.

REFERENCES

Architectural Institute of Japan (1991) "Standard for Structural Calculation of Reinforced Concrete Structures" (in Japanese)

Architectural Institute of Japan et al. (1997) "Report on the Hanshin-Awaji Earthquake Disaster, Structural Damage to Reinforced Concrete Buildings" (in Japanese)

Elwood K J and Moehle J P (2003): "Shake Table Tests on the Axial Load Failure of Reinforced Concrete Columns," *Proceedings of fib Symposium -Concrete Structures in Seismic Regions-*

Ito K, Yoshimura M, and Nakamura T (2011) "Collapse Drift of old Reinforced Concrete Columns," *Summaries of Technical Papers of Annual Meeting*, Architectural Institute of Japan, C-2, pp.163-164 (in Japanese)

Moehle J P, Elwood K J, and Sezen H (2001) "Gravity Load Collapse of Building Frames during Earthquakes," ACI SP-197, *Behavior and Design of Concrete Structures for Seismic Performance*, American Concrete Institute

Nakamura T and Yoshimura M (2003) "Axial Collapse of R/C Short Columns," *Proceedings of fib Symposium - Concrete Structures in Seismic Regions-*, Paper No.159

Nakamura T and Yoshimura M (2012) "Simulation of Old Reinforced Concrete Column Collapse by Pseudo-dynamic Test Method," *Proceedings of the fifteenth World Conference in Earthquake Engineering*

Yoshimura M and Takaine Y (2005) "Evaluation of Vertical Deformation for R/C Columns with Shear Mode Based on Concept of Failure Surface Contraction, " *Journal of Structural and Construction Engineering*, Architectural Institute of Japan, No. 592, pp. 167-175 (in Japanese)

Yoshimura M (2008) "Formulation of Post-peak Behavior of Old Reinforced Concrete Columns until Collapse, " *Proceedings of the fourteenth World Conference in Earthquake Engineering*